Structure and vibrational spectra of small water clusters from first principles simulations

Dongdong Kang, Jiayu Dai, Yong Hou, and Jianmin Yuan[a)]
Department of Physics, National University of Defense Technology, Changsha 410073, People's Republic of China

(Received 5 April 2010; accepted 17 June 2010; published online 7 July 2010)

The structure and vibrational spectra of $(H_2O)_n$ $(n=2-5)$ clusters have been studied based on first-principles molecular dynamics simulations. Trends of the cluster structures with the cluster size show that water molecules in cluster are bound more tightly. The vibrational spectra as a function of cluster size and temperature are obtained using Fourier transformation of the velocity autocorrelation function. Results of the clusters in ground state show that when the cluster size increases, the librational peaks shift to blue and the bonded intramolecular OH stretching bands shift to red due to the clusterization and hydrogen-bond strengthening. Meanwhile, there are no significant shifts in the intramolecular bending and free OH stretching modes, indicating that the free hydrogen atoms are insensitive to the local bonding environment. The temperature-dependent vibrational spectra, which exhibit similar behaviors from the dimer to pentamer, show that there are significant broadenings of the spectra with temperature caused by thermal motions. Moreover, different bands shift to different directions, where librational bands shift to red while bonded OH stretching bands shift to blue, although the blueshifts are quite small for the dimer and trimer.
© *2010 American Institute of Physics*. [doi:10.1063/1.3462278]

I. INTRODUCTION

Water clusters, formed by hydrogen-bonded (H-bonded) water molecules, play prominent roles in many areas, such as biology, chemistry, astrophysics, and environmental science.[1] Long-lived small water clusters are known to exist in water vapor with non-negligible amounts and in the atmosphere at typical atmospheric conditions,[2] and play an important role in the greenhouse effect.[3] Most importantly, water clusters are expected to be the powerful probes to reveal the unique properties of water in various condensed phases.

Water is the most important liquid due to its ubiquity in daily life and significance in many different areas of science.[4,5] Though an enormous amount of effort has been made to explore its peculiar properties in both experiments and theoretical calculations, the nature of water has not been fully understood, which arises mostly from the complex network of highly directional hydrogen bonds (H-bonds) formed by the explicitly simple water molecule.[6] In particular, one of the open issues is the microscopic structure of liquid water. There are two main insights for the structure of liquid water. One is the continuum model with a continuous H-bonded near-tetrahedral network, supported by molecular dynamics (MD) calculations[7,8] and experimental measurements.[9] The other one is the mixture model where the liquid is considered to consist of different regions with different structures (distorted and tetrahedral species) or a mixture of clusters of different sizes.[11] This model was first suggested by Wernet *et al.*[10] from x-ray absorption spectroscopy and x-ray Raman scattering. Moreover, a 2:1 ratio between distorted and tetrahedral species at room temperature was estimated by Nilsson *et al.*[12] In addition, Kashtanov *et al.*[13] reported the x-ray emission spectra of liquid water by simulating water clusters with different sizes and conformations embedded in a continuum medium. Therefore, it can be expected that a few water molecules bonded by H-bonds could provide significant information of the local environment in the bulk liquid water and the knowledge of water clusters is significant for unraveling the structural and dynamical properties of liquid water from molecular level.

A large number of experimental and theoretical studies have been devoted to explore the structural, energetic, and dynamic properties of neutral water clusters[14–17] as well as anionic[18] and protonated[19] water clusters. Behaviors of water clusters in external fields were also reported recently.[20] For neutral water clusters, much attention has been paid to their structures and vibrational spectra in the last decades. Pioneering work on structural information of the water dimer was carried out by Dyke *et al.*,[21] employing molecular beam electric resonance spectroscopy in the radio frequency and microwave ranges. The vibration-rotation-tunneling spectra of small water clusters were extensively studied by Saykally's group,[22,23] who made noticeable efforts to systematically untangle the intricacies associated with cooperative hydrogen bonding. In addition, infrared (IR) spectra, which play a crucial role to understand the structures of water clusters, have been measured by many groups. Coker *et al.*[24] measured the IR predissociation spectra of water clusters in the frequency range of 3000–3800 cm^{-1}. Huisken *et al.*[25] carried out reliable assignment of the IR absorption bands to individual water clusters through mass-selective vibrational predissociation technique. The IR spectra of $(H_2O)_{2-6}$

[a)]Author to whom correspondence should be addressed. Electronic mail: jmyuan@nudt.edu.cn.

 © 2010 American Institute of Physics

Downloaded 23 Sep 2013 to 202.197.9.8. This article is copyrighted as indicated in the abstract. Reuse of AIP content is subject to the terms at: http://jcp.aip.org/about/rights_and_permissions

trapped in solid nitrogen or rare gas matrix have also been measured.[26,27] Miller and Nauta[28] identified the OH spectra of the cyclic water hexamer in liquid helium. With helium droplet technique, the strengths of the IR absorption of small water clusters as a function of size have been measured by Slipchenko *et al.*[29] Recently, Moudens *et al.*[30] presented clear signatures of the free and H-bonded OH vibrations in water aggregates from the dimer to pentamer in their Fourier transform IR measurements. Although all these experimental data have provided the signatures of water clusters, it is difficult to correlate the structural and dynamical properties of these clusters solely through experiments. A combination of theoretical calculations and experimental measurements is necessary to obtain these correlations.[14]

On theoretical side, early investigation was performed for the vibrational spectra of $(H_2O)_{2-4}$ by Honegger and Leutwyler[31] at the self-consistent field level. Since then, there have been extensive theoretical calculations to study water clusters. Lee *et al.*[14] calculated the characteristic trends in various properties of $(H_2O)_{1-10}$ such as structures, energies, vibrational spectra, and electronic properties, which are useful in the assignments of the experimental OH stretching and HOH bending modes. The structures of water clusters with size less than 14 were optimized based on the single-parent genetic algorithm developed by Zhang *et al.*[16] Subsequent investigations were extended to clusters of 30 water molecules.[32,33] Moreover, accurate anharmonic vibrational spectra from the dimer to pentamer were also predicted based on expensive *ab initio* calculations, which can be used to identify different clusters under the correct experimental conditions.[34] Since the calculations above obtained only zero-temperature properties, many MD simulations have been performed to reveal the temperature-dependent properties. Bosma *et al.*[35] simulated the Raman and IR spectra of water clusters in the range of 0–1000 cm^{-1}. The far-IR spectra of small water clusters were calculated by Lee *et al.*[36] by employing first-principles MD simulation, and the result showed that both the cluster size and the temperature affected the spectra significantly. Though the results of these calculations were in comparative agreement with experiments, we must note that many calculations were based on empirical interaction potentials [(e.g., SPC/E,[37] TIP4P,[38] TIP5P,[39] and TTM3-F (Ref. 32)]. The qualities of these calculations depended on the chosen model potentials considerably and were not always adequate. On the other hand, first-principles methods within density functional theory (DFT) have overcome these limitations to large extent, although the current DFT approaches cannot describe the intermolecular dispersion interaction.[8] Especially, Car–Parrinello[40] (CP) MD simulation has become a powerful tool to describe liquid water and water clusters.[41] In the meantime, the accuracy of available DFT exchange-correlation functionals for water clusters was verified in details.[42]

As widely known, notable intensity at a certain frequency in the IR or Raman spectra only indicates the existence of a vibrational state of IR-active or Raman-active, and other vibrational states without these activations are not exhibited in these spectra. Although these vibrational states are very important for analyzing the motional characteristics of the vibrational modes, less attention has been given to them so far. Besides, the dependence on the cluster size and the temperature of the vibrational spectra of water clusters are also less investigated. Therefore, it is helpful to calculate the vibrational spectra of water clusters systematically from first-principles simulations. As a precondition of studying vibrational and other physical properties, the structures of small water clusters are optimized first and the trends of the cluster structures are also investigated in the present work.

II. THEORETICAL METHOD

There are at least two approaches to compute vibrational spectra. One is the straightforward diagonalization of the Hessian matrix evaluated by computing the second derivative of the potential surface, from which one can obtain the normal modes at the ground states only. A more systematic technique is computing the velocity autocorrelation (VAC) function from MD simulation, thus one can obtain the vibrational density of states, presenting peaks at the phonon eigenfrequencies, by the Fourier transform of the VAC function:

$$I(\omega) = 2\int_0^\infty C(t)\cos\,\omega t dt \tag{1}$$

with

$$C(t) \equiv \frac{\langle \mathbf{v}(t_0+t)\cdot\mathbf{v}(t_0)\rangle}{\langle \mathbf{v}^2(t_0)\rangle} = \frac{\Sigma_{j=1}^{n_t}\Sigma_{i=1}^{N}\mathbf{v}_i(t_{0j}+t)\cdot\mathbf{v}_i(t_{0j})}{\Sigma_{j=1}^{n_t}\Sigma_{i=1}^{N}\mathbf{v}_i^2(t_{0j})}, \tag{2}$$

where $\langle\ \rangle$ is the time averaged value calculated along the entire trajectories, N is the number of atoms in a cluster, and n_t is the number of different time origins. In this work, n_t is taken to be 800. Compared to the first approach, the second method cannot only deal with the ground state, but also be competent to tackle the behavior at finite temperatures. Therefore the second method is an important approach for computing temperature-dependent vibrational spectra of small water clusters, although the VAC function is sometimes changed into dipole autocorrelation function to obtain the IR spectra.

In the present study, CPMD simulation, as implemented in the CPMD package,[43] is adopted to investigate the structures and vibrational spectra of water clusters $(H_2O)_n$ $(n=2-5)$. The CP method, which combines the DFT with the classical MD method, is a powerful technique to investigate the structural and vibrational properties of cluster.[44] In the current case, we consider each water cluster as an isolated system and adopt the supercell model. The atoms exhibiting special geometry within clusters are put into the center of a large cubic cell. Periodic boundary conditions are imposed on the large supercell with edges of 10 Å to ensure that there is no appreciable interaction between periodic images. In the DFT framework, we use the Becke–Lee–Yang–Parr[45,46] (BLYP) functional to treat the exchange-correlation interaction between electrons, which has been shown to give a good description of the structural and vibrational properties of small water clusters.[36,41] The interaction between the core and valence electrons is described by Troullier–Martins

Downloaded 23 Sep 2013 to 202.197.9.8. This article is copyrighted as indicated in the abstract. Reuse of AIP content is subject to the terms at: http://jcp.aip.org/about/rights_and_permissions

TABLE I. Structures of the water monomer and water clusters $(H_2O)_n$ $(n=2-5)$. $d(O-O)$, $\phi(H-O-H)$, and $d(O\cdots H)$ denote the OO distance, intramolecular HOH angle, and length of H-bond, respectively. $d(O-H)_b$ denotes the intramolecular OH distance where the hydrogen atom is bonded by H-bond. $d(O-H)_f$ denotes the intramolecular OH distance where the hydrogen atom is free of H-bond. E_b denotes the binding energy. All values are averaged over all the molecules except monomer. Experimental data are given in parentheses. The results of liquid water are from experiments.

n	$d(O-O)$ (Å)	$\phi(H-O-H)$ (degree)	$d(O-H)_b$ (Å)	$d(O-H)_f$ (Å)	$d(O\cdots H)$ (Å)	E_b (meV/mol.)
1		104.5 (104.5[a])		0.974 (0.957[b])		
2	2.96 (2.95[c])	104.8	0.982	0.974	1.983	93.1
3	2.83 (2.85[c])	105.8	0.989	0.973	1.926	195.4
4	2.74 (2.79[c])	105.8	0.999	0.973	1.752	256.1
5	2.73 (2.76[c])	105.9	1.000	0.973	1.729	272.0
Liquid	2.80[d]	106.0[e]	0.970[e]			

[a]Reference 49.
[b]Reference 50.
[c]Reference 22.
[d]Reference 52.
[e]Reference 53.

norm-conserving pseudopotential[47] with a plane-wave cutoff of 90 Ry. The computations are performed at the Γ point only of the Brillouin zone.

We perform first-principles MD simulations of $(H_2O)_n$ $(n=2-5)$ at different temperatures. Verlet algorithm is used to integrate the equations of motion. Taking into account both the efficiency and accuracy of the computation, the time step is taken to be 2 a.u. with the fictitious electronic mass of 100 a.u. This set of parameters provides conservation of the total energy within 10^{-6} Ry and maintains adiabatic conditions for the electrons in the whole MD trajectory. As an isolated system, the initial momentum of cluster is set to be zero and the total angular momentum is also hold to be zero to restrict the cluster rotation. In order to generate an initially equilibrated ensemble at the desired starting temperature, we perform a canonical ensemble simulation of about 1.5 ps where the temperature is controlled by Nosé–Hoover-chain thermostats,[48] then a 10 ps microcanonical MD run is followed as the production simulation. When calculating the vibrational spectra of the clusters with ground-state configurations, the average temperature over the whole trajectory is near the desired value of 10 K. In order to study the changes in the vibrational spectra with temperature, we increase the temperature from about 10 K with an increment of approximate 100 K each time.

III. RESULTS AND DISCUSSION

A. Geometry

There have been many calculations for the ground-state structures of $(H_2O)_n$ $(n=2-5)$. However, there have been small differences between the results of different theoretical approximations. Here we use the structures of $(H_2O)_n$ $(n=2-5)$ clusters optimized in Ref. 42 as the starting geometries of the present MD evolution. The relaxation of the starting geometries to their ground state is carried out using Broyden-Fletcher-Goldfarb-Shano (BFGS) algorithm with a convergence threshold of 10^{-6} a.u. We also calculate the binding energy for each stable structure, which is defined as $E_b(n)=nE[H_2O]-E[(H_2O)_n]$. In order to verify the validity of calculation, we optimize the structure of water monomer first. The results are shown in Table I. One can see that the optimized structure of the water monomer is in nice agreement with experiments.[49,50] Subsequently, we relax the structures of $(H_2O)_n$ $(n=2-5)$ and present the results in Fig. 1. Meanwhile, three additional conformers (Trimer uuu, Tetramer C_i, Tetramer pyramid) are also displayed in Fig. 1, which are obtained with G3 method and predicted to be the significant isomers at 298 K using the Boltzmann distribution equation.[51] It is shown that for each cluster the relaxation is small and the optimized bond lengths are consistent with the values in literature.[22,42] The dimer is an open chain with C_s symmetry while the trimer, tetramer, and pentamer are ring structures with C_1, S_4, and C_1 symmetries, respec-

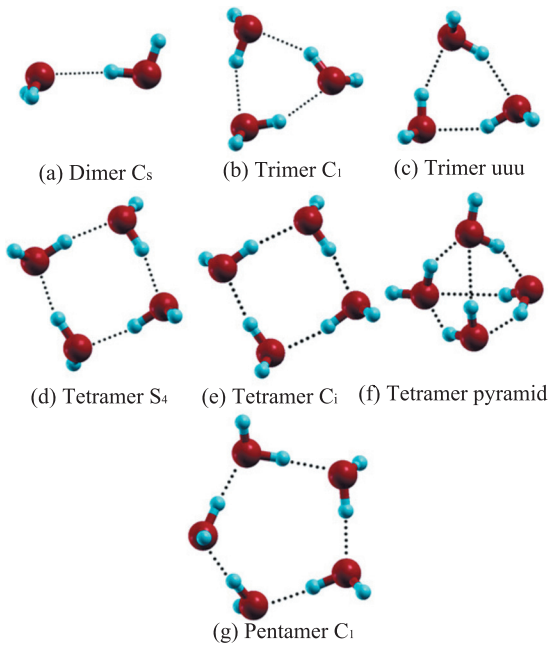

FIG. 1. Structures of $(H_2O)_n$ $(n=2-5)$. (a), (b), (d), and (g) are the ground-state structures of $(H_2O)_n$ $(n=2-5)$, respectively. (c) is one of trimer isomers. (e) and (f) are two tetramer isomers. The dotted lines denote the H-bonds.

Downloaded 23 Sep 2013 to 202.197.9.8. This article is copyrighted as indicated in the abstract. Reuse of AIP content is subject to the terms at: http://jcp.aip.org/about/rights_and_permissions

tively. In spite of some undulations, these ring clusters are nearly planar structures and have one free and one H-bonded OH oscillator per H_2O unit. It should be noted that the dimer exhibits some characteristics different from other clusters, that is, the dimer has only one H-bond, which is less than the number of molecules in cluster, while other clusters have as many H-bonds as their size number. Thus it would be expected that water molecules are bound less tightly in the dimer than bound in other clusters.

In Table I, one can see that the OO distance between adjacent oxygen atoms decreases dramatically from 2.96 to 2.73 Å when the cluster size increases. Similar behavior has also been observed in H-bond length, decreasing from 1.983 to 1.729 Å, whereas the length of the intramolecular OH bond related to the H-bonded hydrogen atom increases gradually with the cluster size. These trends indicate that water molecules are bound more tightly when the cluster size increases, which are also supported by the binding energies listed in Table I. It can also be noted that the intramolecular HOH angle in the dimer almost holds the same value as in the monomer while the trimer, tetramer and pentamer hold a larger value than the dimer and monomer. In addition, the length of the intramolecular OH bond related to the free hydrogen atom also holds the almost same value from the monomer to pentamer. It indicates that the clusterization has nearly no impact on these free hydrogen atoms. Comparing with experimental structural parameters of liquid water shows that the OO distance in liquid water is not the limit of the cluster value with the increasing size, which is larger than that of the tetramer and pentamer. Meanwhile, the OH bond is smaller in liquid water than that in clusters. Only the intramolecular HOH angle in liquid water seems to be the limit of the cluster value. The comparison implies that the clusters embedded in liquid water are much different from gaseous clusters. It can be understood in that a single molecule in small water clusters has highly directional interaction with other molecules, whereas the single molecule in liquid water is influenced by many molecules from various directions. Moreover, the experimental results of liquid water are obtained at room temperature, the thermal fluctuation effect at finite temperature weakens the H-bonds by continually breaking and binding. As a result, for liquid water, the H-bond network is less compact than that in small water clusters and the OH bond length is more close to the value of the water monomer. In Fig. 2, the comparisons of our calculated OO distance with the experimental data[22] and other theoretical results are displayed.[42,54] It is shown that our results of the dimer and trimer are more close to the experimental values while the results of the tetramer and pentamer improve other theoretical calculations nonobviously, indicating that the DFT is powerful but not perfect to deal with the H-bonded clusters.

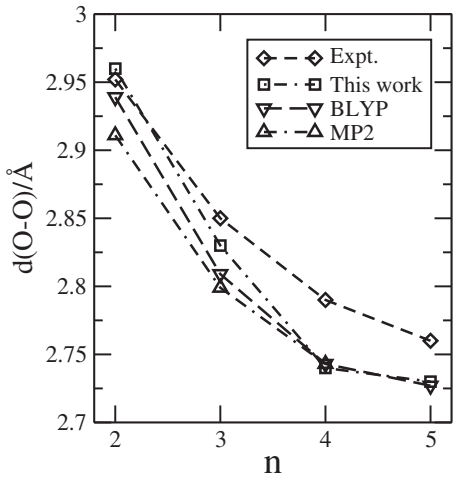

FIG. 2. Comparison of the computed OO distances in water clusters through various methods with the experimental value. The results of BLYP, MP2, and experiment are from Refs .54, 42, and 22, respectively.

B. Vibrational spectra at ground state

At first, the eigenvibrational spectra of the water monomer are calculated to verify the validity of our MD simulations. The normal modes of the water monomer obtained in this work at 10 K are the bending mode at 1581 cm^{-1}, the symmetric stretching mode at 3657 cm^{-1}, and the asymmetric stretching mode at 3754 cm^{-1} in contrast with the experimental values of 1595, 3657, and 3756 cm^{-1}, respectively.[55] It can be seen that our results are in excellent agreement with experiment, indicating the accuracy of our simulations. The eigenvibrational spectra of $(H_2O)_n$ $(n=2-5)$ clusters calculated based on the optimized structures are shown in Fig. 3. Since there are $3n-6$ vibrational degrees of freedom for the cluster with n atoms, the number of vibrational frequencies of normal modes is $3n-6$. As shown in Fig. 3, there are several degenerate normal modes. In order to clarify the degenerate normal modes and check the correctness of the MD simulation, the Hessian matrix obtained by differentiating the Hellmann–Feynman forces with respect to atomic coordinates is diagonalized to give the eigenvibrational frequencies of the ground-state configurations. The results for $(H_2O)_n$ $(n=2-5)$ clusters are shown in Table II in comparison with experimental values. It shows fair agreement between these two theoretical models, with typical differences of about 20 cm^{-1}. Due to the small mass, the quantum features of the hydrogen atom vibrations play an important role in the dynamics of liquid water and water clusters. Classical mechanics cannot describe the motion of proton accurately,[59] par-

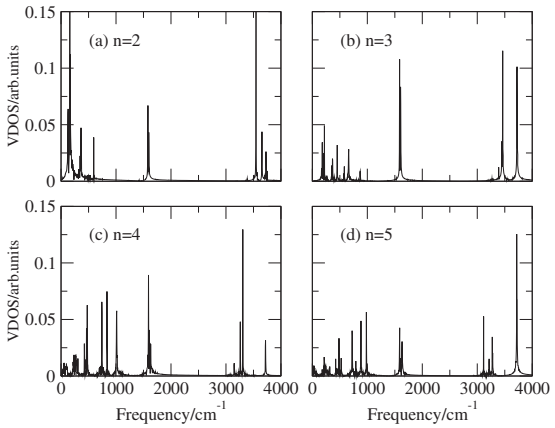

FIG. 3. The calculated vibrational density of states for the ground state $(H_2O)_n$ $(n=2-5)$ clusters.

Downloaded 23 Sep 2013 to 202.197.9.8. This article is copyrighted as indicated in the abstract. Reuse of AIP content is subject to the terms at: http://jcp.aip.org/about/rights_and_permissions

TABLE II. Comparison between the calculated eigenvibrational frequencies of the ground-state water clusters using CPMD simulation and Hessian matrix diagonalization, along with a few available experimental values. Frequencies are given in units of cm^{-1}.

	CP	Hessian	Expt.		CP	Hessian	Expt.		CP	Hessian	Expt.
$n=2$	129	136	93[a]	$n=4$	56	69		$n=5$	71	72	
	160	157	115[a]		98	103	168		94	97	
	168	164	123[a]		219	205			147	127	
	186	201	143[b]		233	228			178	150	
	364	358	311[a]		240	244			202	205	
	594	606	523[a]		247	246			209	213	
	1579	1586	1599[a]		261	269			215	218	
	1597	1604	1617[a]		272	278			232	241	
	3547	3574	3591[a]		282	280			246	246	
	3654	3689	3661[a]		306	318			263	258	
	3728	3766	3734[a]		424	421			276	275	
	3753	3789	3750[a]		456	454			297	300	
$n=3$	166	142			463	467			303	302	
	181	159			476	467			316	311	
	195	167			741	760			424	430	
	212	207			835	838			444	446	
	219	229			835	839			468	470	
	264	257			1011	999			484	481	
	355	361			1580	1593			525	535	
	368	390			1590	1610	1629[e]		724	727	
	451	448			1604	1610			790	796	
	580	576	569[c]		1630	1640			885	872	
	663	681			3150	3192			885	889	
	869	873			3261	3300			982	988	
	1587	1592			3261	3300	3416[d]		1588	1601	
	1604	1601	1609[d]		3306	3342			1605	1614	
	1604	1617	1638[e]		3720	3756			1622	1623	
	3390	3418			3720	3757			1632	1645	
	3449	3482	3533[d]		3720	3757	3714[d]		1639	1652	
	3463	3494			3720	3757			3116	3133	
	3724	3760							3206	3229	
	3724	3761	3726[d]						3216	3237	3353[d]
		3761							3274	3288	
									3280	3297	
									3718	3740	
									3718	3740	
									3718	3742	3717[d]
									3718	3744	
									3718	3746	

[a]Reference 26.
[b]Reference 56.
[c]Reference 57.
[d]Reference 25.
[e]Reference 58.

ticularly at low temperatures. In the present study, quantum features were not taken into account in the process of obtaining the eigenvibrational frequencies. The good agreement between theory and experiment for the eigenvibrational spectra from the monomer to pentamer might be reached because the well-known tendency of DFT to underestimate harmonic frequencies of water just counteracts the quantum effect corrections. Concerning the experimental results, it is difficult to assemble complete gas-phase experimental data in one experiment for all the water clusters discussed, so part of the experimental results listed in Table II are obtained from the matrix measurements. However, these results are quite close to the gas-phase results since the perturbations induced by rare gas matrix are very small.[26] Owing to the lack of enough experimental data, we cannot determine definitely the ground-state structures of $(H_2O)_n$ $(n=2-5)$ optimized in our simulation via comparisons between theory and experiment. Nevertheless, these structures are still the most important candidates for the ground-state configurations of $(H_2O)_n$ $(n=2-5)$ because they have been predicted in many theoretical studies.

As mentioned above, water dimer, including only one H-bond, consists of one proton-acceptor and one proton-donor molecule. The former has three vibration modes of symmetric stretching, bending, and asymmetric stretching,

Downloaded 23 Sep 2013 to 202.197.9.8. This article is copyrighted as indicated in the abstract. Reuse of AIP content is subject to the terms at: http://jcp.aip.org/about/rights_and_permissions

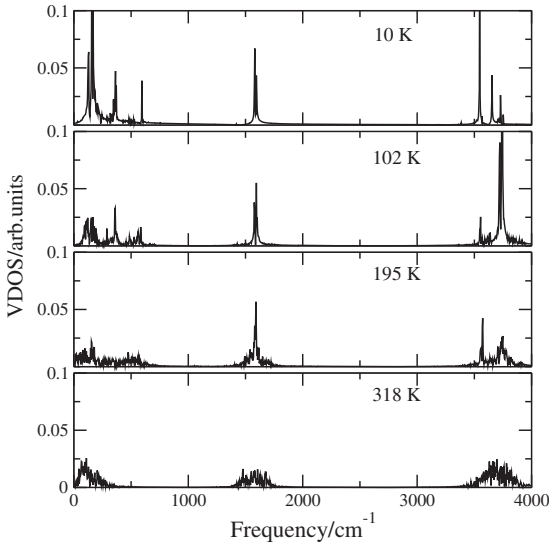

FIG. 4. The calculated vibrational density of states of water dimer at different temperatures.

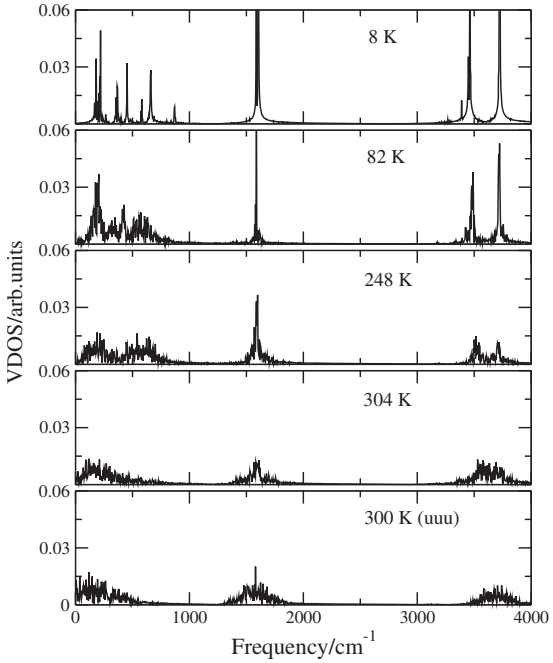

FIG. 5. The calculated vibrational density of states of water trimer at different temperatures. The bottom panel is the result of the uuu trimer at 300 K.

while the latter has three vibrational modes of bending, free OH stretching, and bonded OH stretching. For the cyclic $(H_2O)_n$ clusters with $n=3-5$, the OH stretching vibrations display two groups, the bonded OH stretching bands and the free OH stretching bands. For all $(H_2O)_n$ clusters with $n=2-5$, the bonded OH stretching frequencies are always lower than the free OH bands located around 3720 cm^{-1} as shown in Table II. In addition, there are three types of intermolecular vibrational modes (libration, translation, and torsion) related to the H-bonds below 1000 cm^{-1}. Anyhow, the vibrational spectra shown in Fig. 3 distribute into three frequency bands: the intermolecular vibrational band below 1000 cm^{-1}, the intramolecular bending band within 1500–1700 cm^{-1}, and the intramolecular stretching band above 3000 cm^{-1}. As shown in Fig. 3, the positions of the bonded OH stretching bands show apparent redshifts with increasing cluster size, while the free OH stretching bands show very small cluster shifts. It is consistent well with Lee's calculation.[14] A remarkable feature in Fig. 3 is that libration peaks in the 300–1000 cm^{-1} range[22] shift to higher frequency when the cluster size increases, which is consistent with the result in Ref. 36.

C. Temperature-dependent vibrational spectra of water clusters

The vibrational spectra of the dimer at different temperatures are plotted in Fig. 4. The spectrum at 10 K is the eigenvibrational spectrum discussed above. One can see that the three distinct vibrational bands broaden gradually as the temperature increases. The position of the bending band does not shift, indicating that the temperature has few effect on the intramolecular bending motions. A distinct change in high-frequency bands is that the peak intensities of the bonded OH stretching around 3547 and 3654 cm^{-1} decrease dramatically with rising temperature. Meanwhile, the free OH stretching peaks around 3728 and 3753 cm^{-1} grow rapidly at 102 K and then fall back to the same height of the bonded OH stretching peaks when the temperature continues rising. However, the positions of these bands do not change. It can be understood in that the molecules have more energy to move at higher temperatures, thereby having larger amplitude stretching motions for either bonded or free OH bond. For the dimer, the free OH stretching modes are thermally excited more rapidly than bonded OH, which leads to the rapidly growing peaks at 102 K. Since the H-bonded hydrogen atoms are less bound at high temperatures, the two types of OH stretching bands possess almost the same status and merge to one band at room temperature due to broadening. Besides, the librational peaks around 364 and 594 cm^{-1} (Ref. 34) broaden gradually also as the temperature increases and disappear abruptly near room temperature. The reason, as pointed out in Ref. 22, is probably that the librational motions are the dominant motion for the initial breaking of H-bonds in liquid water as well as water clusters while other intermolecular motions do not lead to significant bond breaking but can indirectly facilitate the breaking by weakening the H-bonds. Therefore, the librational peaks would drop faster than other characteristic peaks along with the H-bonds breaking till they disappear at high temperatures.

In Fig. 5, the vibrational spectra of the ground-state trimer as a function of temperature are given. The vibrational spectrum of uuu trimer at 300 K is also presented. For the C_1 trimer, the features of the spectra are similar to the dimer. One can see that bending bands broaden gradually with increasing temperature, whereas the bonded and free OH stretching bands not only broaden but also shift slightly close to each other. The intermolecular vibrational bands, which have a distinct characteristic at low temperatures, shift to red accompanied by a marked broadening as the temperature increases. Like the dimer, the librational bands of the trimer in the range of 300–1000 cm^{-1} (Ref. 22) also weaken sharply near room temperature due to the fact that H-bonds are

Downloaded 23 Sep 2013 to 202.197.9.8. This article is copyrighted as indicated in the abstract. Reuse of AIP content is subject to the terms at: http://jcp.aip.org/about/rights_and_permissions

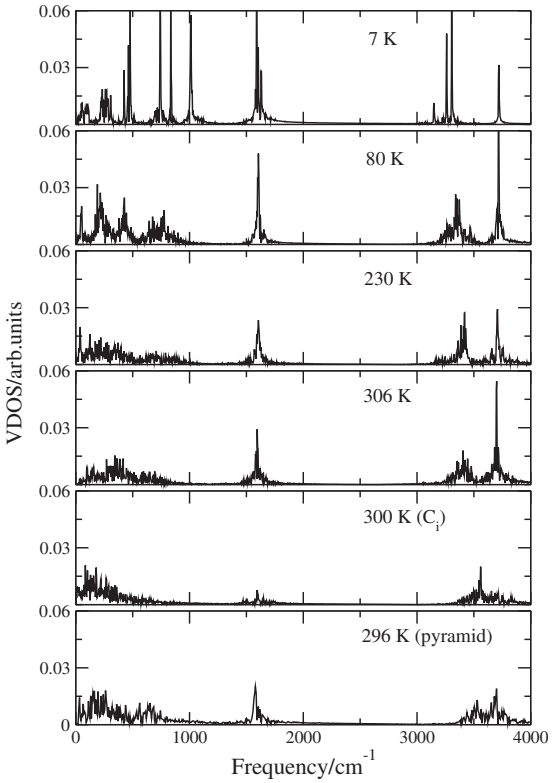

FIG. 6. The calculated vibrational density of states of water tetramer at different temperatures. The bottom two panels are the results of the C_i and pyramid tetramer near room temperature, respectively.

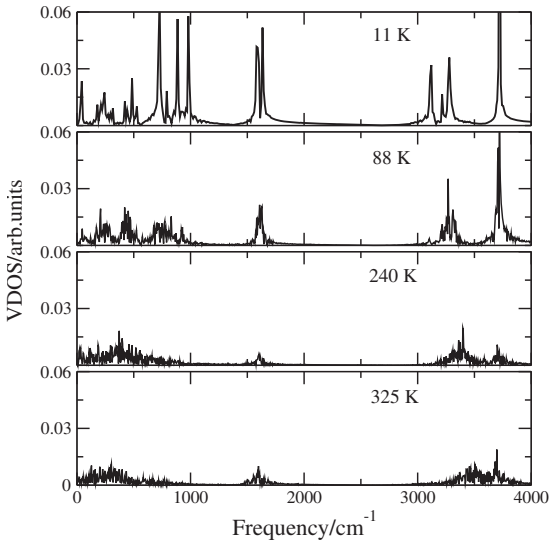

FIG. 7. The calculated vibrational density of states of water pentamer at different temperatures.

weakly bonded (100–300 meV/H bond)[42] and easy to break with thermal fluctuation and rearrangement. The uuu isomer with all dangling hydrogens pointing up on the same side of the ring, as shown in Fig. 1, is one of the two stable cyclic trimers. The uuu isomer is less stable with relative free energy of 0.004 kcal/mol higher than the global minimum configuration with C_1 symmetry at 298 K. The relative free energy difference is so small that the uuu isomer has a large conformational population according to the Boltzmann distribution.[51] In order to learn the contribution of uuu trimer to the vibrational spectra at room temperature, we take the uuu configuration as the initial structure and calculate the vibrational spectrum at 300 K. It can be seen that there is quite small difference between the spectra of the C_1 and uuu trimer. It is indicated that the two conformers have reached equilibrium distribution within the simulation time scale here due to the small difference of the free energy. The relative electronic energy difference of 0.5 kcal/mol (Ref. 51) at 0 K implies that it is difficult to transform between them at low temperatures. Nevertheless, as the temperature increases, the entropic effects begin to dominant the free energies and it comes to transform easily between the trimer isomers.

The vibrational spectra of the ground-state tetramer as well as the C_i and pyramid tetramer are presented in Fig. 6. As discussed by Day *et al.*, the S_4, C_i, and pyramid tetramers are the predominant fraction of the tetramer distribution at 298 K and comprise 51.5%, 33%, and 15.5% of the total number, respectively. It should be noted that DFT methods typically do not locate the pyramid tetramer as a minimum,[60] namely, DFT methods do not accurately describe the potential hypersurface around the minimum point of the pyramid tetramer. However, DFT methods can be competent to describe the finite temperature behavior of the pyramid tetramer because we do not need to deal with the minimum issue in this case. Figure 7 shows the vibrational spectra of the ground-state pentamer. Due to the 95.3% population of C_1 pentamer, we do not consider other conformers of the pentamer. As shown in Figs. 6 and 7, the common feature of the temperature-dependent vibrational spectra of the ground-state tetramer and pentamer is the spectral broadening due to atomic thermal motions with increasing temperature. An important feature, different from the dimer and trimer, is that the bonded OH stretching bands shift to blue as the temperature increases. It means that the temperature has more impact on larger clusters such as the tetramer and pentamer than the small ones such as the dimer and trimer; that is, the dynamics of the H-bonded hydrogen atoms in larger clusters is more sensitive to the temperature effect. Since the redshifts of the bonded OH stretching bands of tetramer and pentamer in ground state are larger than those of the dimer and trimer, more remarkable shifts of the bonded OH stretching bands with increasing temperature are displayed by the spectra of the tetramer and pentamer. From Fig. 6, it can be seen that the spectra of the C_i and pyramid tetramers near room temperature are somewhat different from the ground-state S_4 tetramer. The bonded OH stretching bands of the two isomers shift to higher frequencies than S_4 tetramer. In principle, if these tetramer isomers reach equilibrium distribution at room temperature, the calculated vibrational spectra should include all the contributions of these isomers whichever isomer structure is taken as the starting structure of the molecular dynamical evolution. The results obtained here seem not to prove this principle. In fact, the relative free energy differences of the C_i and pyramid tetramers are 0.26 and 0.71 kcal/mol, respectively, above the S_4 tetramer.[51] Thus these isomers do not reach equilibrium distribution in our simulation time scale (about 10 ps). The vibrational spectra obtained by starting from one specific tetramer are mostly con-

Downloaded 23 Sep 2013 to 202.197.9.8. This article is copyrighted as indicated in the abstract. Reuse of AIP content is subject to the terms at: http://jcp.aip.org/about/rights_and_permissions

tributed by itself. In addition, it should be noted that the bigger the cluster size is, the larger the frequency range covered by the intermolecular vibrational bands at room temperature. The spectra of water clusters seem to approach the vibrational spectra of the bulk liquid water.[15] As we know, liquid water has strong IR absorption below 1000 cm^{-1}, within 1500–1700 cm^{-1}, and 3000–4000 cm^{-1} at room temperature.[15,61] Thus appearance of the corresponding vibrational bands of water clusters in these frequency range near room temperatures may indicate that liquid water consists of different water clusters connected by weak and constantly rearranging H-bonds. The absorption spectra of water are furthermore resulted from the superposition of the contributions of water clusters with various sizes.

IV. CONCLUSION

First-principles MD simulations are carried out to study the temperature-dependent vibrational spectra of $(H_2O)_n$ $(n=2-5)$ clusters based on the tightly optimized structures. Observing the trends of structural parameters of water clusters such as OO distance, intramolecular H-bonded OH distance and binding energy, it is deduced that water molecules in small clusters are bound more tightly by H-bonds when the cluster size gets bigger. Comparisons of the calculated structural parameters of water clusters with the experimental value of liquid water show that the local environment in liquid water is somewhat different from clusters. Distinct features of vibrational spectra of water clusters at ground state are presented. When the cluster size increases, the librational peaks shift to blue while the intramolecular bonded OH stretching bands shift to red. It is the result of clusterization and H-bond strengthening. In addition, since the free hydrogen atoms are insensitive to the local bonding environment, there is no significant shift in the intramolecular bending and free OH stretching modes. The vibrational spectra of $(H_2O)_n$ $(n=2-5)$ clusters as a function of temperature present similar behaviors. As the temperature increases, the vibrational spectra broaden gradually. Meanwhile, different bands shift to different directions, where librational bands shift to red and bonded OH stretching bands shift to blue, although the blueshifts are quite small for the dimer and trimer.

ACKNOWLEDGMENTS

This work was supported by the National Natural Science Foundation of China under Grant Nos. 10734140, 60921062, and 10676039 and the National Basic Research Program of China (973 Program) under Grant No. 2007CB815105. Calculations are carried out at the Research Center of Supercomputing Application, NUDT.

[1] A. Michaelides and K. Morgenstern, Nature Mater. **6**, 597 (2007).
[2] K. Pfeilsticker, A. Lotter, C. Peters, and H. Bösch, Science **300**, 2078 (2003).
[3] P. F. Bernath, Phys. Chem. Chem. Phys. **4**, 1501 (2002).
[4] X. R. Wang and H. P. Zheng, Chin. Phys. B **18**, 1968 (2009).
[5] Z. K. Gao and N. D. Jin, Chin. Phys. B **18**, 5249 (2009).
[6] P. Ball, Nature (London) **452**, 291 (2008).
[7] P. L. Silvestrelli and M. Parrinello, J. Chem. Phys. **111**, 3572 (1999).
[8] R. Bukowski, K. Szalewicz, G. C. Groenenboom, and A. van der Avoird, Science **315**, 1249 (2007).
[9] A. Hermann, W. G. Schmidt, and P. Schwerdtfeger, Phys. Rev. Lett. **100**, 207403 (2008).
[10] Ph. Wernet, D. Nordlund, U. Bergmann, M. Cavalleri, M. Odelius, H. Ogasawara, L. Å. Näslund, T. K. Hirsch, L. Ojamäe, P. Glatzel, L. G. M. Pettersson, and A. Nilsson, Science **304**, 995 (2004).
[11] C. Huang, K. T. Wikfeldt, T. Tokushima, D. Nordlund, Y. Harada, U. Bergmann, M. Niebuhr, T. M. Weiss, Y. Horikawa, M. Leetmaa, M. P. Ljungberg, O. Takahashi, A. Lenz, L. Ojamae, A. P. Lyubartsev, S. Shin, L. G. M. Pettersson, and A. Nilsson, Proc. Natl. Acad. Sci. U.S.A. **106**, 15214 (2009).
[12] T. Tokushima, Y. Harada, O. Takahashi, Y. Senba, H. Ohashi, L. G. M. Pettersson, A. Nilsson, and S. Shin, Chem. Phys. Lett. **460**, 387 (2008).
[13] S. Kashtanov, A. Augustsson, Y. Luo, J.-H. Guo, C. Såthe, J.-E. Rubensson, H. Siegbahn, J. Nordgren, and H. Ågren, Phys. Rev. B **69**, 024201 (2004).
[14] H. M. Lee, S. B. Suh, J. Y. Lee, P. Tarakeshwar, and K. S. Kim, J. Chem. Phys. **112**, 9759 (2000).
[15] S. Habershon, G. S. Fanourgakis, and D. E. Manolopoulos, J. Chem. Phys. **129**, 074501 (2008).
[16] S. L. Zhang, H. S. Chen, Y. Song, and Y. H. Yin, Acta Phys. Sin. **56**, 2553 (2007).
[17] H. S. Chen, F. S. Meng, X. F. Li, and S. L. Zhang, Acta Phys. Sin. **58**, 0887 (2009).
[18] L. Ma, K. Majer, F. Chirot, and B. von Issendorff, J. Chem. Phys. **131**, 144303 (2009).
[19] H. B. Yu and Q. Cui, J. Chem. Phys. **127**, 234504 (2007).
[20] R. Moro, R. Rabinovitch, C. L. Xia, and V. V. Kresin, Phys. Rev. Lett. **97**, 123401 (2006).
[21] T. R. Dyke, K. M. Mack, and J. S. Muenter, J. Chem. Phys. **66**, 498 (1977).
[22] F. N. Keutsch and R. J. Saykally, Proc. Natl. Acad. Sci. U.S.A. **98**, 10533 (2001).
[23] H. A. Harker, F. N. Keutsch, C. Leforestier, Y. Scribano, J. X. Han, and R. J. Saykally, Mol. Phys. **105**, 497 (2007).
[24] D. F. Coker, R. E. Miller, and R. O. Watts, J. Chem. Phys. **82**, 3554 (1985).
[25] F. Huisken, M. Kaloudis, and A. Kulcke, J. Chem. Phys. **104**, 17 (1996).
[26] Y. Bouteiller and J. P. Perchard, Chem. Phys. **305**, 1 (2004).
[27] S. Hirabayashi and K. M. T. Yamada, J. Chem. Phys. **122**, 244501 (2005).
[28] K. Nauta and R. E. Miller, Science **287**, 293 (2000).
[29] M. N. Slipchenko, K. E. Kuyanov, B. G. Sartakov, and A. F. Vilesov, J. Chem. Phys. **124**, 241101 (2006).
[30] A. Moudens, R. Georges, M. Goubet, J. Makarewicz, S. E. Lokshtanov, and A. A. Vigasin, J. Chem. Phys. **131**, 204312 (2009).
[31] E. Honegger and S. Leutwyler, J. Chem. Phys. **88**, 2582 (1988).
[32] G. S. Fanourgakis and S. S. Xantheas, J. Chem. Phys. **128**, 074506 (2008).
[33] A. Lenz and L. Ojamäe, J. Phys. Chem. A **110**, 13388 (2006).
[34] M. E. Dunn, T. M. Evans, K. N. Kirschner, and G. C. Shields, J. Phys. Chem. A **110**, 303 (2006).
[35] W. B. Bosma, L. E. Fried, and S. Mukamel, J. Chem. Phys. **98**, 4413 (1993).
[36] M. S. Lee, F. Baletto, D. G. Kanhere, and S. Scandolo, J. Chem. Phys. **128**, 214506 (2008).
[37] H. J. C. Berendsen, J. R. Grigera, and T. P. Straatsma, J. Phys. Chem. **91**, 6269 (1987).
[38] W. L. Jorgensen, J. Chandrasekhar, J. D. Madura, R. W. Impey, and M. L. Klein, J. Chem. Phys. **79**, 926 (1983).
[39] M. W. Mahoney and W. L. Jorgensen, J. Chem. Phys. **112**, 8910 (2000).
[40] R. Car and M. Parrinello, Phys. Rev. Lett. **55**, 2471 (1985).
[41] J. Grossman, E. Schwegler, E. W. Draeger, F. Gygi, and G. Galli, J. Chem. Phys. **120**, 300 (2004).
[42] B. Santra, A. Michaelides, and M. Scheffler, J. Chem. Phys. **127**, 184104 (2007).
[43] CPMD version 3.13.2, http://www.cpmd.org/, Copyright IBM Corp 1990–2008, Copyright MPI für Festkörperforschung Stuttgart 1997–2001.
[44] D. D. Kang, Y. Hou, J. Y. Dai, and J. M. Yuan, Phys. Rev. A **79**, 063202 (2009).
[45] A. D. Becke, Phys. Rev. A **38**, 3098 (1988).
[46] C. Lee, W. Yang, and R. G. Parr, Phys. Rev. B **37**, 785 (1988).
[47] N. Troullier and J. Martins, Phys. Rev. B **43**, 1993 (1991).

Downloaded 23 Sep 2013 to 202.197.9.8. This article is copyrighted as indicated in the abstract. Reuse of AIP content is subject to the terms at: http://jcp.aip.org/about/rights_and_permissions

[48] G. J. Martyna, M. L. Klein, and M. Tuckerman, J. Chem. Phys. **97**, 2635 (1992).
[49] S. A. Clough, Y. Beers, G. P. Klein, and L. S. Rothman, J. Chem. Phys. **59**, 2254 (1973).
[50] W. S. Benedict, N. Gailar, and E. K. Plyler, J. Chem. Phys. **24**, 1139 (1956).
[51] M. B. Day, K. N. Kirschner, and G. C. Shields, J. Phys. Chem. A **109**, 6773 (2005).
[52] J. A. Odutola and T. R. Dyke, J. Chem. Phys. **72**, 5062 (1980).
[53] K. Ichikawa, Y. Kameda, T. Yamaguchi, H. Wakita, and M. Misawa, Mol. Phys. **73**, 79 (1991).
[54] S. S. Xantheas, J. Chem. Phys. **102**, 4505 (1995).
[55] L. S. Rothman, R. R. Gamache, R. H. Tipping, C. P. Rinsland, M. A. H. Smith, D. C. Benner, V. M. Devi, J.-M. Flaud, C. Camy-Peyret, A. Perrin, A. Goldman, S. T. Massie, L. R. Brown, and R. A. Toth, J. Quant. Spectrosc. Radiat. Transf. **48**, 469 (1992).
[56] F. N. Keutsch, L. B. Braly, M. G. Brown, H. A. Harker, P. B. Petersen, C. Leforestier, and R. J. Saykally, J. Chem. Phys. **119**, 8927 (2003).
[57] J. Ceponkus, G. Karlstrom, and B. Nelander, J. Phys. Chem. A **109**, 7859 (2005).
[58] J. B. Paul, C. P. Collier, R. J. Saykally, J. J. Scherer, and A. O'Keefe, J. Phys. Chem. A **101**, 5211 (1997).
[59] L. Ojamäe and K. Hermansson, Chem. Phys. Lett. **191**, 500 (1992).
[60] V. S. Bryantsev, M. S. Diallo, A. C. T. van Duin, and W. A. Goddard III, J. Chem. Theory Comput. **5**, 1016 (2009).
[61] J. E. Bertie and Z. Lan, Appl. Spectrosc. **50**, 1047 (1996).

Downloaded 23 Sep 2013 to 202.197.9.8. This article is copyrighted as indicated in the abstract. Reuse of AIP content is subject to the terms at: http://jcp.aip.org/about/rights_and_permissions